

# Semipolar r-plane ZnO films on Si(100) substrates: Thin film epitaxy and optical properties

Ravi Aggarwal,<sup>1</sup> Honghui Zhou,<sup>1</sup> Chunming Jin,<sup>2</sup> J. Narayan,<sup>1</sup> and Roger J. Narayan<sup>1,2,a)</sup>

<sup>1</sup>*Department of Materials Science and Engineering, North Carolina State University, Raleigh, North Carolina 27695, USA*

<sup>2</sup>*Joint Department of Biomedical Engineering, University of North Carolina, Chapel Hill, North Carolina 27599, USA*

(Received 10 March 2010; accepted 24 March 2010; published online 9 June 2010)

We report heteroepitaxial growth of (10 $\bar{1}2$ ) oriented (r-plane) ZnO films on Si(100) substrates. The films were grown by pulsed laser deposition and integration of ZnO with silicon was achieved using a tetragonal yttria stabilized zirconia (YSZ) buffer layer. It was observed that ZnO films grown at temperatures in the range of 700–750 °C with relatively high oxygen pressure ( $\sim 70$  mTorr) were (10 $\bar{1}2$ ) oriented. ZnO films deposited with lower oxygen pressures were found to be purely (0002) orientated. Experiments carried out to elucidate the role of oxygen pressure indicated that the crystallographic orientation of ZnO depends on the nature of atomic termination of YSZ layer. It has been proposed that crystallographic orientation of ZnO is controlled by chemical free energy associated with ZnO-YSZ interface. Detailed x-ray diffraction and transmission electron microscopy studies showed existence of four types of in-plane domains in r-plane ZnO films. Optical characterization demonstrated that photoluminescence of r-plane ZnO films was superior to that of c-plane ZnO films grown under similar conditions. © 2010 American Institute of Physics. [doi:10.1063/1.3406260]

## I. INTRODUCTION

Zinc oxide is a wide band gap semiconductor with significant potential for use in ultraviolet optoelectronic devices such as light emitting diodes and lasing devices.<sup>1,2</sup> ZnO has hexagonal wurtzite structure and has a preference to grow along the [0001] direction (c-axis). Along the c-axis, zinc and oxygen layers alternate, imparting a polar character to (0001)-oriented wurtzite ZnO. The piezoelectric and the polarity-induced electrostatic fields in (0001) oriented wurtzite materials lead to spatial separation of electrons and holes, thereby, reducing the radiative recombination probability. This impairs the light emitting efficiency of devices built with (0001)-oriented wurtzite active layers.<sup>3</sup> One approach to overcome this limitation is to grow ZnO in nonpolar orientations in which polarization is zero.<sup>4</sup> This has lead to considerable research on the growth and characterization of two nonpolar orientations of ZnO, a-plane (11 $\bar{2}0$ ) and m-plane (10 $\bar{1}0$ ).<sup>5–7</sup> The polarization effects can also be minimized by growing wurtzite materials in semipolar orientations. In recent years, there has been significant interest in growing GaN and other wurtzite nitride materials in semipolar orientations for optoelectronic devices.<sup>8–10</sup> In these semipolar orientations, the polarization effects are minimal and higher amounts of dopants (e.g., indium in GaN) can be incorporated compared to nonpolar orientations. Since ZnO has similar crystal structure and properties to GaN, the semipolar orientations of ZnO are also expected to exhibit optoelectronic properties that are desirable for device applications.

However, there has been little work on semipolar orientations of ZnO. The main reason for this is the strong tendency of ZnO to grow in polar c-orientation on most substrates, while very specific substrates and deposition conditions are required to grow nonpolar or semipolar orientations of ZnO. One of the most important semipolar orientations in ZnO is (10 $\bar{1}2$ ), which is referred to as the r-plane. As established for GaN, polarization effects are expected to be very small for r-plane oriented ZnO.<sup>11</sup> In this paper, we present a novel approach to grow semipolar r-plane ZnO films. We demonstrate that r-plane ZnO films can be integrated with the easily available and technologically important Si(100) substrate.

In an earlier work, we have shown that tetragonal yttria stabilized zirconia (YSZ) can be grown epitaxially on Si(100) substrates using pulsed laser deposition. Further, we had demonstrated heteroepitaxial growth of polar c-plane ZnO films on YSZ buffered Si(100) substrates.<sup>12</sup> In the present paper, we show that semipolar r-plane orientation of ZnO can be epitaxially grown on YSZ buffered Si(100) by controlling the deposition conditions. It has been shown that the growth orientation of ZnO on YSZ buffered silicon depends on the nature of atomic termination of YSZ layer, which is controlled by oxygen pressure. We have carried out detailed x-ray diffraction (XRD) and transmission electron microscopy (TEM) investigations to assess the structural details of the films. The photoluminescence (PL) spectra for r-plane ZnO films have been compared with those for c-ZnO films grown under similar conditions.

## II. EXPERIMENTAL DETAILS

YSZ buffer layer and ZnO films were grown on Si(100) substrates using KrF excimer pulsed laser deposition ( $\lambda = 248$  nm). Prior to deposition, silicon substrates were ultra-

<sup>a)</sup>Author to whom correspondence should be addressed. UNC-NCSU, Joint Department of Biomedical Engineering, 3143 Burlington Engineering Laboratories, Campus Box 7115, Raleigh, NC 27695-7115. Tel.: 919 696 8488. FAX: 919 513 3814. Electronic mail: rjnaraya@unity.ncsu.edu.

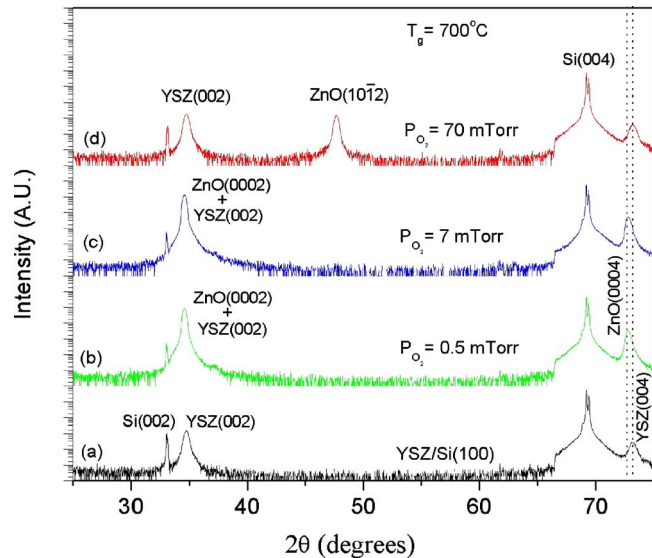


FIG. 1. (Color online) XRD  $\theta$ - $2\theta$  scan data for (a) YSZ/Si(100) heterostructure and [(b)–(d)] ZnO/YSZ/Si(100) heterostructures grown at different oxygen partial pressures. The ZnO growth temperature was 700 °C for all the samples.

sonically cleaned with acetone and methanol. High-purity YSZ (5 mol %— $\text{Y}_2\text{O}_3$  doped  $\text{ZrO}_2$ ) and ZnO targets were used for the deposition. The energy density used in this study was  $\sim 3 \text{ J/cm}^2$ . A target-substrate distance of 4.5 cm and a pulse rate of laser of 5 Hz were utilized. The growth temperature was maintained at 800 °C for deposition of YSZ layer. ZnO growth was done at 700, 750, or 800 °C. To remove the oxide layer on silicon, 400 pulses of YSZ were deposited in vacuum. Oxygen was subsequently introduced in the chamber. 600 pulses of YSZ were then deposited at an oxygen partial pressure of 0.5 mTorr. After adjusting the substrate temperature to ZnO growth temperature, 6000 pulses of ZnO were deposited. Growth of ZnO was performed at three different oxygen partial pressures in the range of 0.5–70 mTorr. XRD studies were done using X'Pert PRO MRD HR x-ray diffractometer (Philips, Eindhoven, the Netherlands) with  $\text{Cu K}\alpha$  radiation. Cross-sectional samples of the ZnO/YSZ/Si(100) heterostructures were characterized using 2000FX and 2010F high resolution transmission electron microscopes (JEOL, Tokyo, Japan). PL spectroscopy of the as-grown samples was done at room temperature using an F-2500 fluorescence spectrophotometer (Hitachi, Tokyo, Japan).

### III. RESULTS AND DISCUSSION

In the first set of the experiments, growth of ZnO films on YSZ buffered Si(100) was investigated at three different oxygen partial pressures at a fixed ZnO growth temperature of 700 °C. The XRD data for the reference YSZ/Si(100) sample and the ZnO/YSZ/Si(100) samples is shown in Fig. 1. The XRD pattern in Fig. 1(a) shows that tetragonal YSZ grows only in the (002) orientation. The XRD patterns for ZnO/YSZ/Si(100) samples in Fig. 1 show that ZnO grows solely in (0002) orientation at lower oxygen partial pressures (0.5 and 7 mTorr). In contrast, at an oxygen partial pressure of 70 mTorr, ZnO grows only in the (10 $\bar{1}2$ ) orientation; no

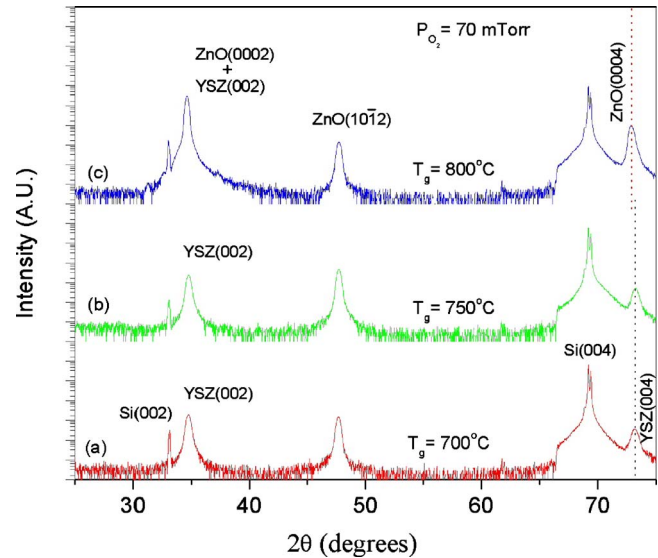


FIG. 2. (Color online) XRD  $\theta$ - $2\theta$  scan data for ZnO/YSZ/Si(100) heterostructures grown at different ZnO growth temperatures. Oxygen partial pressure was 70 mTorr for all of the samples.

other orientation of ZnO is present [Fig. 1(d)]. It should be noted that YSZ (002) and ZnO (0002) peaks are very close and it may seem difficult to index them unambiguously. However, this ambiguity can be removed by looking at the second order peaks, which have larger separation, and also by comparing the intensities of YSZ (002) and ZnO (0002) peaks. The ZnO (0002) peaks are around 100 times more intense than YSZ (002) peak, for which intensity is expected to remain unchanged as YSZ deposition conditions were identical for all of the samples. We have also examined the effect of temperature on growth behavior of ZnO on the YSZ buffer by fixing the oxygen partial pressure at 70 mTorr. The XRD data for these samples is shown in Fig. 2. It was observed that ZnO grows only in the (10 $\bar{1}2$ ) orientation at 700 and 750 °C. However, (0002) orientation of ZnO was also present along with (10 $\bar{1}2$ ) orientation for ZnO grown at 800 °C. Hence, it can be concluded that (10 $\bar{1}2$ ) orientation is favored over (0002) orientation at low temperatures and high oxygen partial pressures.

The oxygen pressure dependence of crystallographic orientation for oxide thin films deposited by pulsed laser deposition has been previously reported in the literature.<sup>13–16</sup> This change in crystallographic orientation of oxides is often attributed to either changes in stoichiometry (which alter the strain energy associated with nonstoichiometric point defects) or decreased kinetic energy of the ablated species with increasing oxygen pressure.<sup>14,15</sup> However, the mechanism underlying this phenomenon is unclear. To understand the role of oxygen pressure in controlling the crystallographic orientation of ZnO, we deposited films where first few pulses of ZnO were deposited at high pressure (70 mTorr, a condition in which ZnO grows only in r-plane orientation). The remainder of the ZnO deposition was continued at lower oxygen pressure (0.5 mTorr, a condition in which ZnO grows only in the c-plane orientation). The XRD results for these samples are summarized in Fig. 3. The XRD results indicate

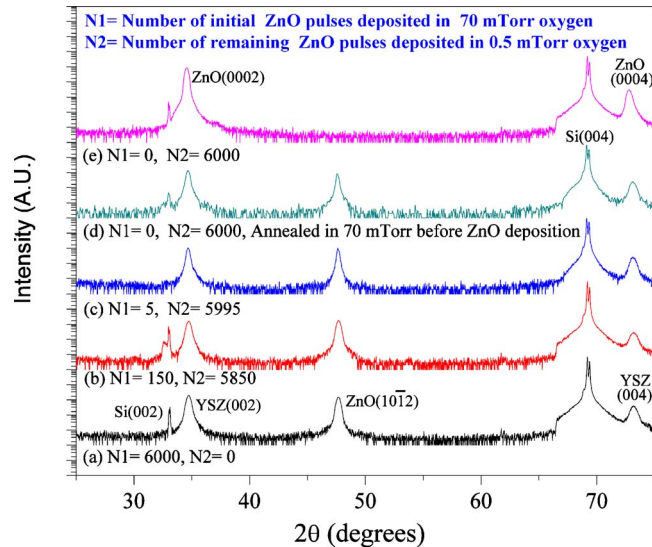


FIG. 3. (Color online) XRD data for ZnO/YSZ/Si(100) heterostructures for which the initial  $N_1$  number of ZnO pulses were deposited at a high oxygen pressure of 70 mTorr and the remaining  $N_2$  (6000- $N_1$ ) pulses were deposited at a reduced oxygen pressure of 0.5 mTorr.

that growth orientation of ZnO is r-plane even if only first five pulses ( $\sim 6$  Å, based on TEM results) of ZnO are deposited in high oxygen pressure, while the rest of the pulses are deposited at low oxygen pressure. This finding indicates that high oxygen pressure is important only for the nucleation stage of r-plane ZnO. Once nucleated, r-plane ZnO can grow even at low oxygen pressures. To understand whether kinetics of the ablated species plays a role in controlling the orientation, one deposition was performed in which the sample was annealed in 70 mTorr oxygen after YSZ deposition for two minutes. The oxygen pressure was subsequently reduced to 0.5 mTorr; all of the pulses of ZnO were then deposited at 0.5 mTorr. The orientation of ZnO in this case also was found to be r-plane. This indicates that kinetics of ablated particles does not affect the crystallographic orientation of ZnO since the entire ZnO deposition was carried out at 0.5 mTorr oxygen partial pressure, a condition in which ZnO prefers to grow in c-plane orientation. This result also indicates that oxygen pressure condition just before the deposition of ZnO, rather than that during the deposition of ZnO, is the key factor that controls the crystallographic orientation of ZnO. This can be explained on the basis of different atomic termination of YSZ layer under different oxygen pressure conditions. We propose that at low oxygen pressures the YSZ surface is Zr-terminated while at higher oxygen pressures surface the YSZ surface is O-terminated. The experimental evidence suggests that c-plane ZnO growth is favored on Zr-terminated YSZ, while r-plane ZnO growth is favored on O-terminated YSZ. To further correlate ZnO orientation with atomic termination of YSZ, we have simulated atomic arrangements of YSZ (002), ZnO (0002), and ZnO (10 $\bar{1}2$ ) planes. These atomic arrangements are shown in Fig. 4. From this figure it can be seen that in YSZ, Zr-only, and O-only layers alternate along [002]. Although Zr-layers are atomically smooth, O-layers are atomically rough. In c-plane ZnO, Zn-only, and O-only layer alternate along a

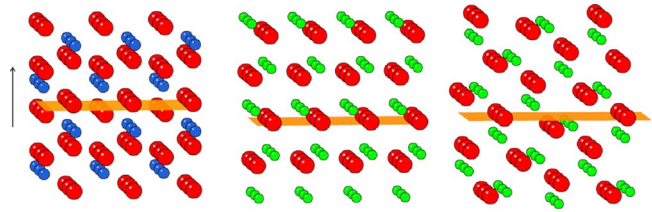


FIG. 4. (Color online) Three-dimensional views of atomic arrangement on (a) YSZ (002) (b) ZnO (0002) and (c) ZnO (10 $\bar{1}2$ ) planes. Planes are shown in shade and the arrow points along the respective plane normals. The larger spheres in (a), (b), and (c) represent oxygen atoms. The smaller spheres in (a) represent Zr atoms. The smaller spheres in (b) and (c) represent Zn atoms. It can be seen that planes defining oxygen atoms are atomically rough for YSZ (002) and ZnO (10 $\bar{1}2$ ) and are atomically smooth for ZnO (0002). Planes defining metal atoms are smooth for both YSZ (002) and ZnO (0002) and are atomically rough for ZnO (10 $\bar{1}2$ ).

direction normal to (0002). Both of these planes are atomically smooth. The atomic arrangement in ZnO (10 $\bar{1}2$ ) plane is more complex, with the planes defining both O and Zn atoms being atomically rough. When YSZ layer is Zr-terminated and is thus atomically smooth, it is likely that first atomic layer of ZnO will be atomically flat O atoms, which is the case for c-plane ZnO. This explains the growth of c-plane orientation of ZnO in low oxygen pressure conditions. On the other hand, when YSZ is O-terminated and is thus atomically rough, the first atomic layer of ZnO is also likely to be atomically rough, which is the case for r-plane ZnO. This explains the growth of r-plane orientation of ZnO in high oxygen pressure conditions. The coexistence of r-plane and c-plane orientations in ZnO films deposited at 800 °C with high oxygen pressure [Fig. 2(c)] can be explained by the mixed termination of YSZ under these conditions. In thin film growth, crystallographic orientation of the film is determined by interplay of chemical energy, which depends on the bonding characteristics across substrate-film interface, and the substrate-film misfit strain energy. The chemical energy for the YSZ-ZnO film interface, for a particular orientation of ZnO, depends on the nature of termination of YSZ layer. However, for a given orientation of ZnO, the strain energy will remain same irrespective of the nature of termination of YSZ layer. Thus, the dependence of orientation of ZnO on nature of termination of YSZ layer indicates that chemical energy, rather than strain energy, is controlling the crystallographic orientation of ZnO on YSZ.

The in-plane orientations of YSZ and ZnO layers in ZnO/YSZ/Si(100) heterostructure was established by XRD  $\phi$ -scans. The  $\phi$ -scan data for a r-plane ZnO/YSZ/Si(100) heterostructure is shown in Fig. 5(a). The  $\phi$ -scan for YSZ layer was done at  $2\theta=30.25^\circ$  and  $\psi=54.2^\circ$ , which corresponds to (101) peak of tetragonal YSZ. The fourfold symmetry seen in the  $\phi$ -scan of YSZ confirms that it is epitaxial and tetragonal. Also, it can be seen that YSZ (101) peaks are at  $45^\circ$  from Si (202) peaks. Hence, the epitaxial relationship of YSZ with silicon substrates can be written as:  $[110]_{\text{YSZ}} \parallel [100]_{\text{Si}}$  and  $(001)_{\text{YSZ}} \parallel (001)_{\text{Si}}$ . This observation is consistent with our previous results.<sup>6</sup> The  $\phi$ -scan for ZnO layer was done at  $2\theta=36.39^\circ$  and  $\psi=18.5^\circ$ , which correspond to the (10 $\bar{1}1$ ) peak of zinc oxide. The  $\phi$ -scan of ZnO



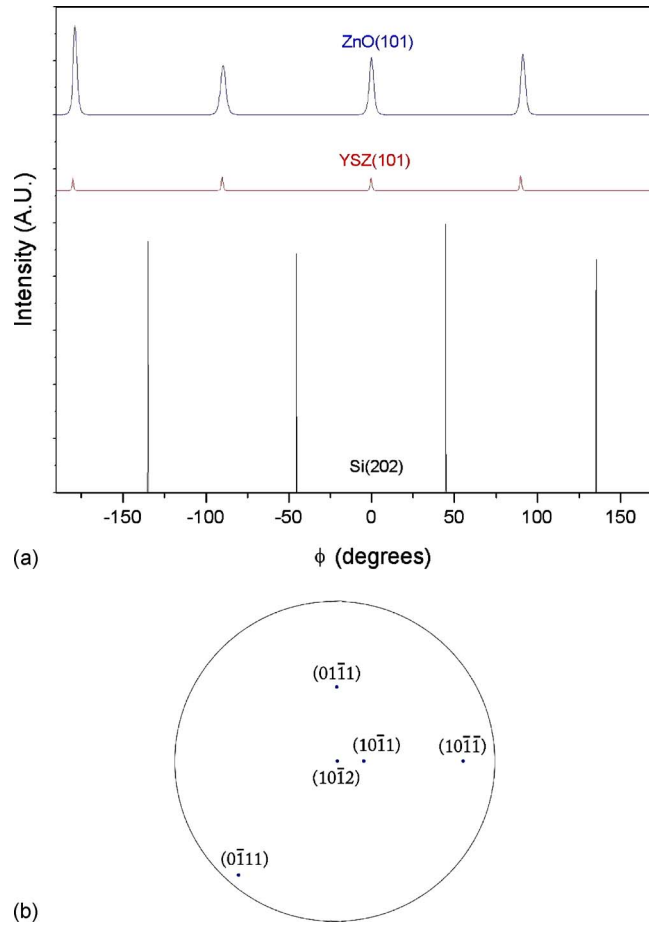


FIG. 5. (Color online) (a) XRD  $\phi$ -scan data for one of the ZnO/YSZ/Si(100) heterostructure. The ZnO growth temperature was 750 °C, while the oxygen partial pressure was 70 mTorr. (b) Calculated stereographic projection of  $\{10\bar{1}1\}$  planes on  $(10\bar{1}2)$  plane for single crystalline ZnO.

shows four peaks which are 90° apart. This indicates that ZnO grows epitaxially on YSZ. The calculated stereographic projection of  $\{10\bar{1}1\}$  planes on  $(10\bar{1}2)$  plane for single crystalline ZnO is shown in Fig. 5(b). From this stereographic projection, it can be concluded that in single crystalline ZnO,  $\{101\}$  planes should exhibit only one-fold symmetry. Hence, the observation of four peaks in  $\phi$ -scan indicates that ZnO has four different in-plane orientations. The position of YSZ (101) peak and ZnO  $(10\bar{1}1)$  peak at the same angle in the  $\phi$ -scan indicates that  $[11\bar{2}0]$  direction of ZnO is parallel to  $[100]$  or  $[010]$  directions of YSZ. The  $[100]$  and  $[010]$  directions in YSZ are equivalent. Thus there are two equally likely orientations of r-ZnO, which are at 90° to each other. These two orientations of ZnO are schematically shown in Fig. 6(a). Here, it should be noted that the atomic arrangement on r-plane of ZnO can be represented by a rectangular lattice, one side of which is along  $[11\bar{2}0]$  while other side is along  $[10\bar{1}1]$  direction. The existence of other two peaks in the  $\phi$ -scan of ZnO can be explained by considering the orientation of c-plane with respect to r-plane of ZnO. The c-plane is inclined at 42.8° with respect to r-plane. The inclination of c-plane can be on either side, which gives rise to two additional orientations of r-plane ZnO; this is schematically shown in Fig. 6(b). As seen from this figure, these two

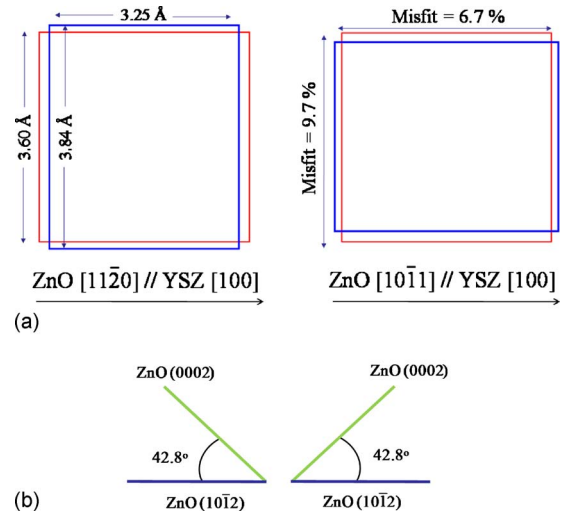


FIG. 6. (Color online) (a) Schematic showing (a) two possible orientations of rectangular r-plane ZnO (dark color) on square (001) plane of YSZ (light color) (b) other two orientation of ZnO, which arise because the c-plane of ZnO can be inclined on either side with respect to the r-plane.

orientations are 180° rotated with respect to each other. Based on this information, the epitaxial relationship for r-ZnO can be written as

$$[11\bar{2}0]_{\text{ZnO}} \text{ or } [10\bar{1}1]_{\text{ZnO}} \parallel [100]_{\text{YSZ}}$$

$$\text{and } (10\bar{1}2)_{\text{ZnO}} \parallel (001)_{\text{YSZ}}.$$

These results were further confirmed using TEM. Figure 7 shows an overview TEM image of the ZnO/YSZ/Si(100) heterostructure and an electron diffraction pattern. The thickness of YSZ layer can be estimated as ~45 nm and the thickness of the ZnO layer can be estimated as ~800 nm from this image. The indexing of electron diffraction pattern shows that spots from ZnO correspond to  $[100]$  and  $[121]$

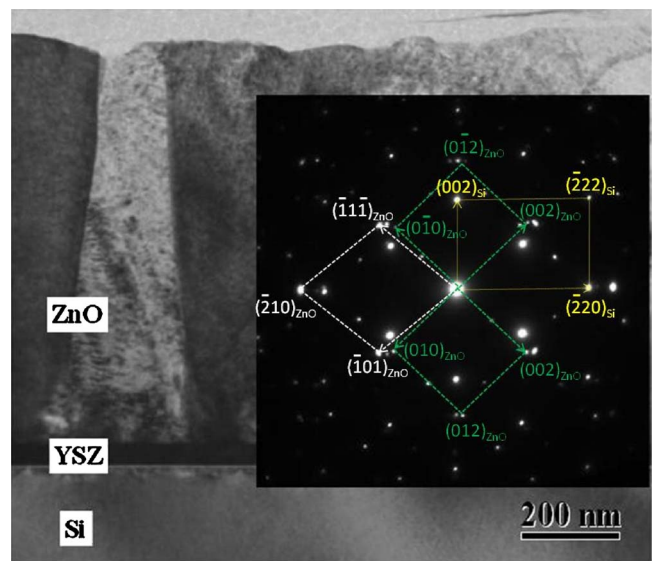


FIG. 7. (Color online) An overview TEM image from a cross-section sample of r-plane ZnO/YSZ/Si(100) heterostructure grown at 700 °C at 50 mTorr oxygen pressure. The inset shows the electron diffraction pattern obtained from all three layers. The YSZ spots are very close to the Si spots and are not indexed to maintain the clarity.

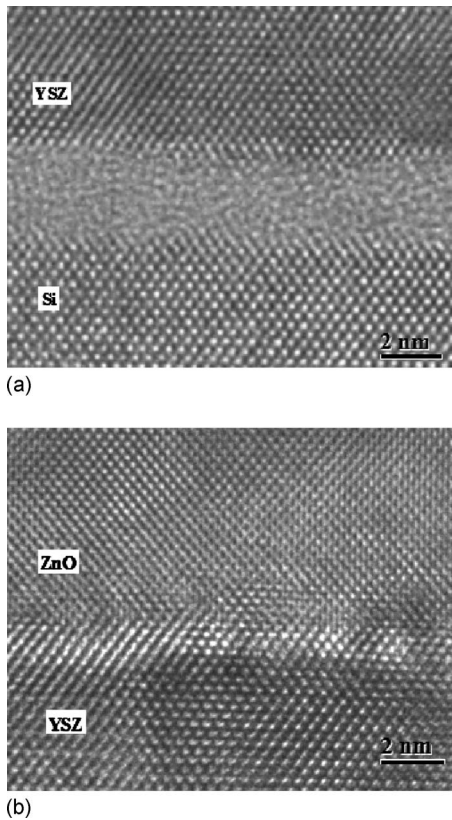


FIG. 8. High resolution TEM images from (a) YSZ/Si(100) interface and (b) ZnO/YSZ interface from a cross-section sample of r-plane ZnO/YSZ/Si(100) heterostructure grown at 700 °C at 50 mTorr oxygen pressure. In these images, Si, YSZ, and ZnO are in [110], [100], and [121] zones, respectively.

zones of ZnO. It should be noted that two variants of [100] zone of ZnO, which are rotated by  $\sim 86^\circ$  from each other, are observed in the electron diffraction pattern. This corresponds to orientation variants of ZnO shown in Fig. 6(b). The electron diffraction pattern also shows that (10 $\bar{1}$ 2) planes of ZnO are tilted by  $\sim 2^\circ$  from (004) planes of Si. The high resolution images of Si/YSZ and YSZ/ZnO interfaces are shown in Fig. 8. In these images, YSZ is in [100] zone while ZnO is in [121] zone. The high resolution image of YSZ/ZnO surface shows that interface is very sharp; no reaction layer at the interface was observed. In the high resolution image of YSZ/Si interface, a  $\sim 2$  nm thick amorphous layer can be observed. As reported earlier, the YSZ layer grows epitaxially on Si(100); this amorphous layer forms during the later stages (after oxygen is introduced in the chamber) of YSZ and ZnO growth as a result of oxygen diffusion to the YSZ/Si interface.<sup>12</sup>

It can be seen from Fig. 6(a) that misfit between r-plane ZnO and tetragonal YSZ is 9.7% in one direction and 6.7% in the perpendicular direction. Epitaxy with such large misfits can be explained in the framework of domain matching epitaxy, in which matching of planes instead of matching of lattice is considered.<sup>17</sup> Along the [11 $\bar{2}$ 0] direction of ZnO, 9.7% misfit can be completely accommodated by two type of domains. In one domain, 10 ZnO planes match 9 YSZ planes. In the other domain, 11 ZnO planes match 10 YSZ planes. The misfit will be completely relaxed if these do-

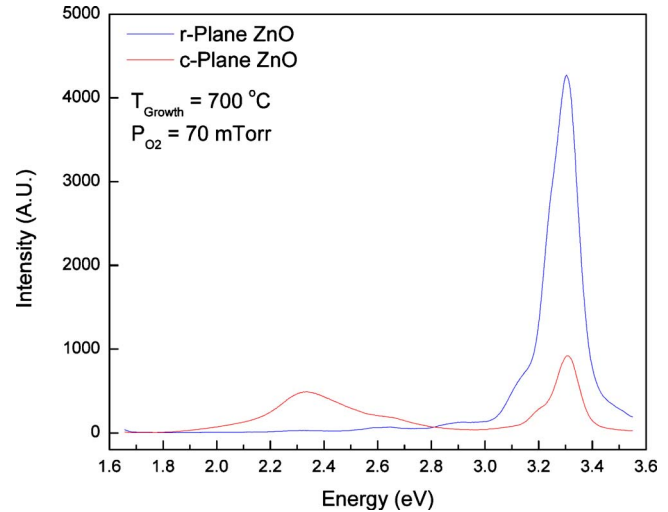


FIG. 9. (Color online) PL spectra of r-plane ZnO/YSZ/Si(100) and c-plane samples deposited at similar conditions. The first 50 pulses of ZnO for c-ZnO were deposited at low oxygen pressure of 0.5 mTorr to nucleate the c-orientation of ZnO.

main alternate with a relative frequency of 5:2. Along the [10 $\bar{1}$ 1] direction of ZnO, 6.7% misfit can be accommodated by a single domain in which 15 ZnO planes match 16 YSZ planes.

The room temperature PL spectra for r-plane ZnO/YSZ/Si(100) and c-plane ZnO/YSZ/Si(100) samples grown under similar conditions are shown in Fig. 9. Both of these spectra exhibit near band emission at 3.3 eV. This near band emission in ZnO is attributed to excitonic recombination.<sup>18</sup> The excitonic emission in r-plane ZnO is approximately five times stronger than that in c-plane ZnO. The stronger excitonic emission observed in r-ZnO can be attributed to the higher probability of radiative recombination in r-plane ZnO due to reduced polarization effects. Another important feature in the spectra shown in Fig. 9 is the prominent broad emission band in c-ZnO, which peaks at 2.35 eV. This emission, termed as green band emission, is often attributed to mid gap point defect levels such as charged oxygen vacancies or zinc interstitials.<sup>19,20</sup> It is interesting to note that green band emission is completely suppressed for r-plane ZnO, which indicates that the density of defects responsible for green band emission is minimal in these films. The reduced green band in r-ZnO films can also contribute to stronger excitonic emission observed in r-ZnO films since the probability of excitonic recombination is increased because of reduced mid gap states. The strong excitonic emission, with negligible emission in visible range, in r-plane ZnO indicates the good optical quality of these films.

#### IV. SUMMARY

To summarize, we have demonstrated heteroepitaxial growth of semipolar r-plane zinc oxide films on YSZ buffered Si(100) substrates. It was found that on YSZ buffered silicon, ZnO grows in r-plane orientation at a high oxygen pressure of 70 mTorr. On the hand, the ZnO films deposited at lower oxygen pressures were c-plane oriented. It is envisaged that the chemical free energy dominates strain free en-

ergy in controlling the orientation of ZnO on YSZ. The oxygen pressure dependence of crystallographic orientation of ZnO films has been explained by considering the nature of atomic termination of YSZ layer. Detailed XRD and TEM studies indicated that r-plane ZnO films exhibited four in-plane orientations. The epitaxial relationship of r-plane ZnO with YSZ buffer layer was established to be:  $[10\bar{1}0]_{\text{ZnO}} \parallel [100]_{\text{YSZ}}$  or  $[01\bar{1}1]_{\text{ZnO}} \parallel [100]_{\text{YSZ}}$  and  $(10\bar{1}2)_{\text{ZnO}} \parallel (001)_{\text{YSZ}}$ . The r-plane ZnO films showed strong excitonic emission, which is indicative of good optical quality.

## ACKNOWLEDGMENTS

This work was supported by the National Science Foundation (Grant Nos. 0547491 and 0921517) and the National Institutes of Health.

<sup>1</sup>U. Özgür, Y. I. Alivov, C. Liu, A. Teke, M. A. Reshchikov, S. Dogan, V. Avrutin, S. J. Cho, and H. Morkoc, *J. Appl. Phys.* **98**, 041301 (2005).

<sup>2</sup>A. Tsukazaki, M. Kubota, A. Ohtomo, T. Onuma, K. Ohtani, H. Ohno, S. F. Chichibu, and M. Kawasaki, *Jpn. J. Appl. Phys., Part 2* **44**, L643 (2005).

<sup>3</sup>M. Leroux, O. Brandt, N. Grandjean, M. Lügt, J. Massies, B. Gil, P. Lefebvre, and P. Bigenwald, *Phys. Rev. B* **58**, R13371 (1998).

<sup>4</sup>P. Waltereit, O. Brandt, A. Trampert, H. T. Grahn, J. Menniger, M. Ramsteiner, M. Reiche, and K. H. Ploog, *Nature (London)* **406**, 865 (2000).

<sup>5</sup>C. R. Gorla, N. W. Emanetoglu, S. Liang, W. E. Mayo, Y. Lu, M. Wra-back, and H. Shen, *J. Appl. Phys.* **85**, 2595 (1999).

<sup>6</sup>T. Moriyama and S. Fujita, *Jpn. J. Appl. Phys., Part 1* **44**, 7919 (2005).

<sup>7</sup>E. Cagin, J. Yang, W. Wang, J. D. Phillips, S. K. Hong, J. W. Lee, and J. Y. Lee, *Appl. Phys. Lett.* **92**, 233505 (2008).

<sup>8</sup>R. Sharma, P. M. Pattison, H. Masui, R. M. Farrell, T. J. Baker, B. A. Haskell, F. Wu, S. P. DenBaars, J. S. Speck, and S. Nakamura, *Appl. Phys. Lett.* **87**, 231110 (2005).

<sup>9</sup>M. Funato, M. Ueda, Y. Kawakami, Y. Narukawa, T. Kosugi, M. Takahashi, and T. Mukai, *Jpn. J. Appl. Phys., Part 2* **45**, L659 (2006).

<sup>10</sup>A. Tyagi, H. Zhong, N. N. Fellows, M. Iza, J. S. Speck, S. P. DenBaars, and S. Nakamura, *Jpn. J. Appl. Phys., Part 2* **46**, L129 (2007).

<sup>11</sup>T. Takeuchi, A. Amano, and I. Akasaki, *J. Appl. Phys.* **39**, 413 (2000).

<sup>12</sup>R. Aggarwal, C. Jin, P. Pant, J. Narayan, and R. J. Narayan, *Appl. Phys. Lett.* **93**, 251905 (2008).

<sup>13</sup>T. Zhao, F. Chen, H. Lu, G. Yang, and Z. Chen, *J. Appl. Phys.* **87**, 7442 (2000).

<sup>14</sup>J. S. Speck, A. Seifert, W. Pompe, and R. Ramesh, *J. Appl. Phys.* **76**, 477 (1994).

<sup>15</sup>C. Li, D. Cui, Y. Zhou, H. Lu, Z. Chen, D. Zhang, and F. Wu, *Appl. Surf. Sci.* **136**, 173 (1998).

<sup>16</sup>C. Wang, B. L. Cheng, S. Y. Wang, H. B. Lu, Y. L. Zhou, Z. H. Chen, and G. Z. Yang, *Thin Solid Films* **485**, 82 (2005).

<sup>17</sup>J. Narayan and B. C. Larson, *J. Appl. Phys.* **93**, 278 (2003).

<sup>18</sup>Y. W. Heo, D. P. Norton, and S. J. Pearton, *J. Appl. Phys.* **98**, 073502 (2005).

<sup>19</sup>K. Vanheusden, W. L. Warren, C. H. Seage, D. R. Tallent, J. A. Voigtang, and B. E. Gnade, *J. Appl. Phys.* **79**, 7983 (1996).

<sup>20</sup>S.-H. Jeong, B.-S. Kim, and B.-T. Lee, *Appl. Phys. Lett.* **82**, 2625 (2003).